Road Resistance of Large Transport Trucks

J. W. ANDERSON, J. C. FIREY, and W. C. KIELING
Respectively, Assistant Professor, Professor, and Assistant Professor of Mechanical Engineering, University of Washington

A road test procedure, using coastdown tests at various loads, has been developed for measuring separately the air drag and tire drag force of a truck. The rayon cord tires tested showed a drag force of 8.2 lb per 1,000-lb load, as measured by these coastdown tests, and a drag force of 8.25 lb per 1,000-lb load as measured by tire dolly towing tests, indicating that the coastdown procedure yields essentially correct results. Air drag coefficients measured by the coastdown test procedure for the four different truck-trailer combinations tested varied between 0.8 and 1.2, being relatively constant for any one truck and trailer. These drag coefficients are of the same order or magnitude as those measured for truck models in wind tunnel tests by Flynn and Kyropoulos (1).

Because the air drag coefficients of full-scale trucks have not previously been measured, other comparisons of the foregoing results cannot be made. To fill in this gap, tests are currently under way to measure the air drag coefficients of full-scale trucks using a railway flat car train as a moving test bed.

•THE DEVELOPMENT of road test procedures for measuring the components of truck rolling resistance and some data obtained by using these procedures are reported. These studies were undertaken to improve the truck fuel consumption and travel time estimation procedures developed by Sawhill and Firey (2) As these estimation procedures were being developed it became evident that a significant source of uncertainty and error in the fuel consumption and travel time estimation method was the lack of general knowledge about the rolling resistance properties of trucks. Sawhill and Firey used an essentially empirical relation for truck rolling resistance which could not be used with confidence for trucks other than those tested. Hence, these studies were undertaken to develop a general relation for truck rolling resistance that could be used to estimate the fuel consumption and travel time for hypothetical future trucks and highways as well as present trucks and highways. In this manner the fuel consumption and travel time procedures may become more useful for highway economic analyses and designs.

The studies are incomplete because independent, non-road test methods of measuring air drag force and bearing and gear drag force are to be developed and compared with the road test results. These further studies will be reported subsequently.

NOMENCLATURE

The following abbreviated nomenclature will be used herein. Indicated in parentheses is the corresponding nomenclature as used by SAE (10).

G = Percent grade of a highway = 100 (Rise)/Distance, (GP);
GVW = Gross vehicle weight in lb, (GW);

Paper sponsored by Committee on Vehicle Characteristics.

A_F = Vehicle frontal area in sq ft, (A);
F = Force in lb;
F_{AD} = Air drag force of tire dolly in lb;
F_M = Measured force in lb;
ρ_a = Air density in pcf;
V = Vehicle speed in fps;
mph = Vehicle speed in miles per hour, (MPH);
g = Gravitational constant in ft/sec/sec;
C_D = Air drag coefficient;
F_T = Tire drag force in lb;
KE = Vehicle kinetic energy in ft-lb;
t = Time in sec;
T = Time in hr;
F_D = Total vehicle drag force in lb;
W = Number of wheels on vehicle;
RHP = Road horsepower, the power required to overcome total drag force, F_D, (Resistance Power);
f_t = Specific tire drag force = 1,000 F_T/GVW;
F_A = Air drag force in lb;
I = Wheel polar moment of inertia in lb-in.-sq sec;
p = Torsional oscillation period in sec;
K = Torsional spring constant in lb-in. per radian;
Θ = Torsional oscillation amplitude in radians;
Φ = Angle of tire tread deflection in radians;
l = Length of tire tread flattened portion in ft;
r = Tire tread radius in ft;
c = Tire tread elastic constant in psf per radian;
b = Tire tread width in ft;
d = Tire tread thickness in ft;
h = Tire tread hysteresis coefficient, the fraction of tread deflection work lost to internal hysteresis;
A_t = Area of the flattened portion of the tire tread in sq ft;
P_i = Tire inflation pressure in psf;
a = Ratio of tire tread flattened area to product of length and width of the flattened portion;
dQ/dt = Rate of heat transfer from the external tire area;
A_X = External tire area in sq ft;
T_t = Tire air temperature in ° F;
T_a = Ambient air temperature in ° F;
ΔT_t = T_t - T_a in ° F = Tire air temperature rise above ambient air temperature;
U = Over-all heat transfer coefficient from tire external area to ambient air temperature, ft-lb/° F/sec/sq ft; and
R = Damping coefficient.

EXPERIMENTAL PROCEDURE

Four types of experiments were carried out: (a) tire dolly towing tests to measure tire drag force; (b) truck towing tests to measure total rolling resistance force; (c) coastdown tests at various loads to measure total rolling resistance force, tire drag force and air drag force; and (d) wheel tests with a torsional spring to measure wheel kinetic energy and improve the accuracy of the coastdown tests.

Road tests were run on a 4-lane portion of US 99 extending about 10 mi north from the town of Marysville, Wash. Four northbound and four southbound test sections of uniform grade were selected and marked with stakes. The grades of these eight sections were then measured with a surveying level and chain (Table 1).

Two trucks and two semitrailers were used in combinations to give four different test vehicles: (a) truck-tractor with gasoline engine, 12 ft wheelbase, single drive axles; (b) truck-tractor with diesel engine, 10 ft 3 in. wheelbase, dual drive axles;

TABLE 1

GRADE OF TEST SECTIONS

Test Section	Direction	Grade (%)
1N	Northbound	0.314[a]
2N	Northbound	0.281[a]
3N	Northbound	0.325[a]
4N	Northbound	0.438[a]
1S	Southbound	0.502[b]
2S	Southbound	0.255[b]
3S	Southbound	0.312[b]
4S	Southbound	0.283[b]

[a]Up. [b]Down.

(c) flatbed semitrailer, 35 ft length, dual rear axles; and (d) van semitrailer, 35 ft length, dual rear axles.

The gasoline-engine truck assembled with the flatbed trailer is shown in Figure 1 and the diesel-engine truck assembled with the van trailer is shown in Figure 2. The diesel-powered truck-trailer combinations have 18 tires of 10:00-20 size. The gasoline-powered truck-trailer combinations have 14 tires of 10:00-20 size. The frontal areas of the four truck-trailer combinations are: gasoline tractor-flatbed trailer, 49.7 sq ft; gasoline tractor-van trailer, 92.9 sq ft; diesel flatbed trailer, 61.4 sq ft; diesel tractor-van trailer, 90.5 sq ft.

Variations in gross vehicle weight were obtained by loading on leased lead pigs securely fastened to the trailer bed. The lead pigs were so small that very little change of frontal area occurred for the flatbed trailer. A Washington State Highway Patrol truck weighing station was used to measure the weights of the test vehicles.

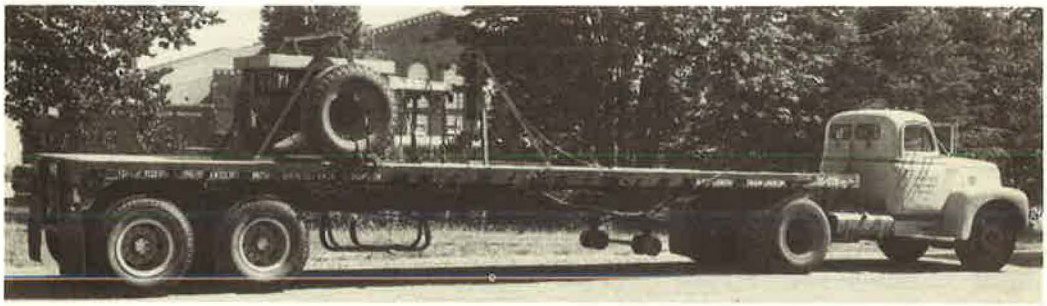

Figure 1. Gasoline tractor with flatbed trailer.

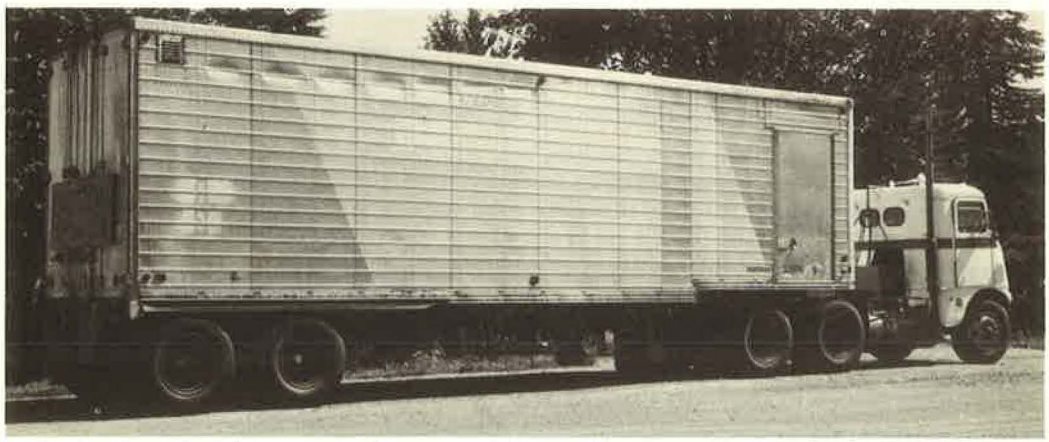

Figure 2. Diesel tractor with van trailer.

Tire Dolly Towing Tests

A separate trailer dolly was used as the tire dolly with two identical test tires mounted in the outer two of the four rims. The dolly was connected to the towing truck by the bracket shown in Figures 3 and 4, which insured that only the force component parallel to road surface was measured by the strain gage towbar. The bracket also provided a safety catch to retain the dolly if the rather delicate strain gage towbar broke. The dolly was fitted with steel brackets and clamps to hold the steel plates, which constituted the tire loading, centrally between the tires. Various numbers and thicknesses of steel plates were used to obtain five different tire loads up to the rated maximum load of the test tires (Table 2). The assembled tire dolly and towing truck are shown in Figure 5.

The valve core was removed from the tire tube valve stem and the stem was fitted with a special tee (Fig. 6). Through this tee an iron-constantan thermocouple was inserted into the tire air space and the side connection was made to a calibrated pressure gage at the wheel hub. The thermocouple leads were connected to a quick-connect fitting. In this manner the prevailing tire air pressure and temperature could be quickly measured after stopping. Tire tread temperatures were measured with a surface pyrometer fitted with a needle thermocouple.

During the tire dolly towing tests particular care was taken to hold a steady speed without acceleration or deceleration by keeping both the speedometer and engine tachom-

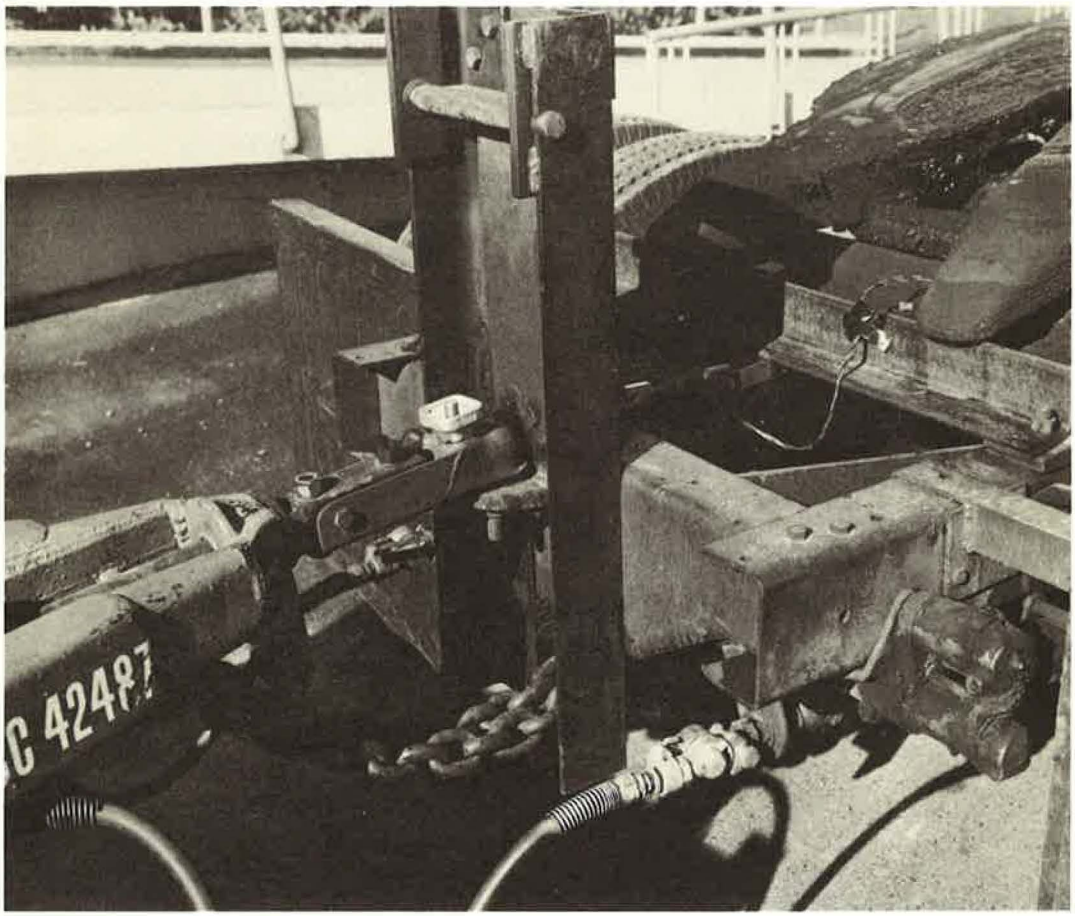

Figure 3. Towing test setup.

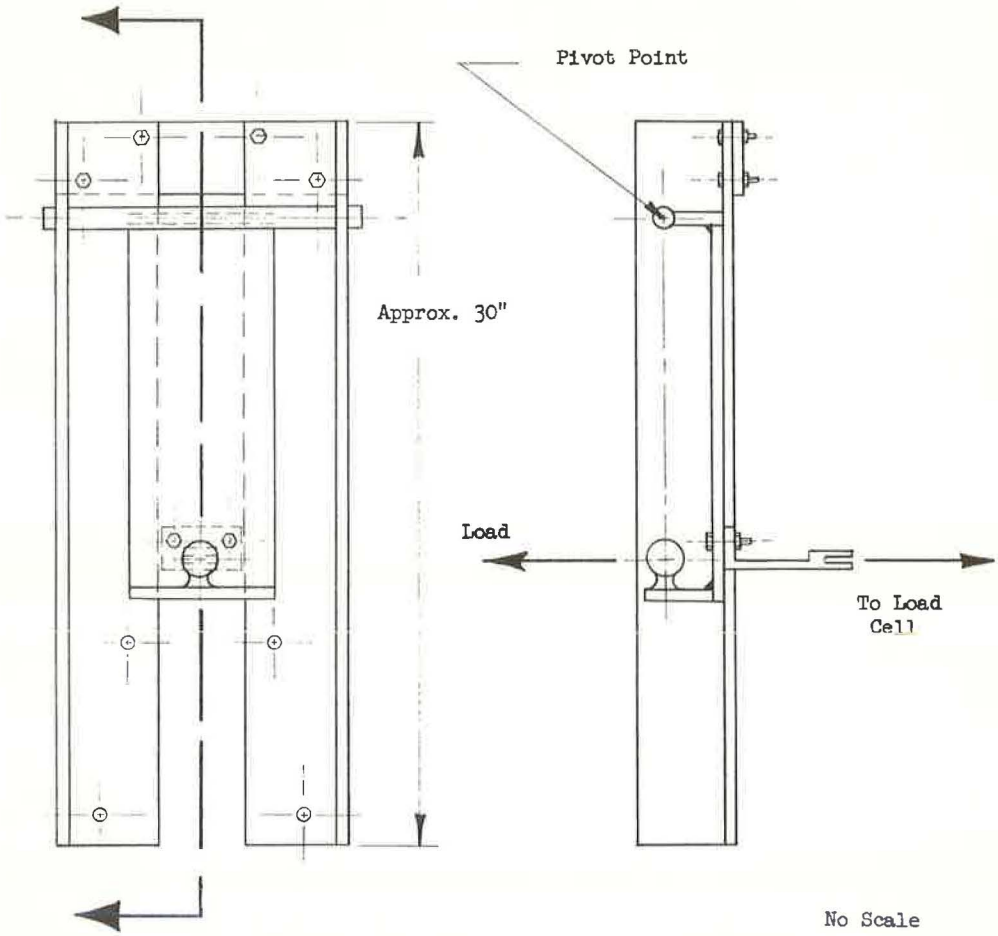

Figure 4. Towing bracket.

TABLE 2

TIRE DOLLY TOWING TEST LOADS

Load	Total Dolly Weight (lb)	Load per Tire (lb)
Empty	2,600	1,300
Quarter	4,100	2,050
Half	5,615	2,807
Three-quarter	7,500	3,750
Full	9,200	4,600

eter at constant readings. For each test condition of load and speed, tire air pressures, tire air temperatures, tread temperatures, and ambient air temperature were recorded before and after each northbound and southbound run. The towbar readings were taken only on the staked test sections of known grade.

Two types of 10:00-20 truck tires were tested, a 12-ply, rayon cord tire and a composite cord tire (steel cords in the carcass and nylon cords in the tread). Only the rayon cord tires were used in the coasting tests.

It was originally hoped that the air drag force of the dolly would be so small that it could be neglected in calculating the tire drag force. However, because this was not the case, it became necessary to measure separately the air drag force of the tire dolly. This was done by suspending the tire dolly from long vertical cables above a flatbed truck and using the towing bracket and strain gage towbar to measure the force between the tire dolly and the flatbed truck as the latter was driven at various steady speeds. This arrangement is shown in Figure 1.

Four resistance wire strain gages were mounted on the towbar made of type 6061-T6 aluminum alloy (Fig. 7). A bridge type strain gage indicating unit was connected to these four

Figure 5. Tire dolly test rig.

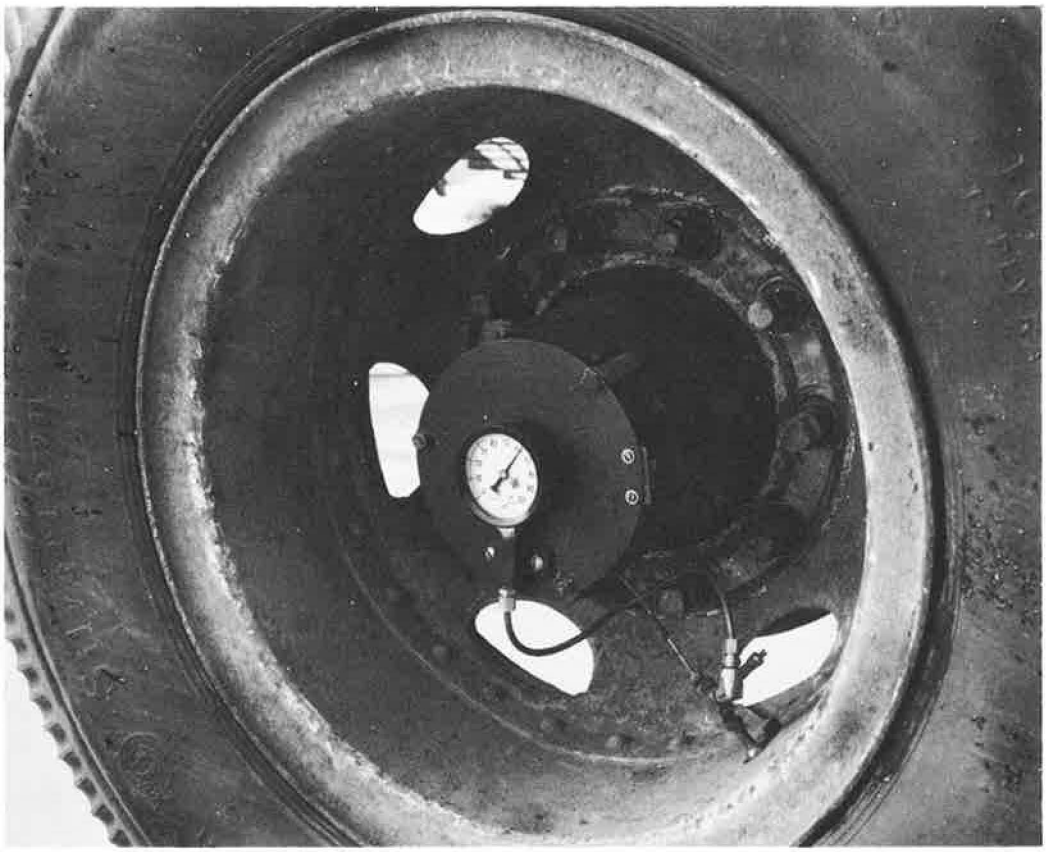

Figure 6. Tire instrumentation.

strain gages (Fig. 8). High sensitivity to strain was obtained and correction was made for thermal expansion of the towbar.

The strain gage towbar was calibrated by suspending known weights by the towbar and recording the resulting change in the strain indicator reading. This change increased linearly with applied weight and the towbar force was calculated as the product of the change in strain

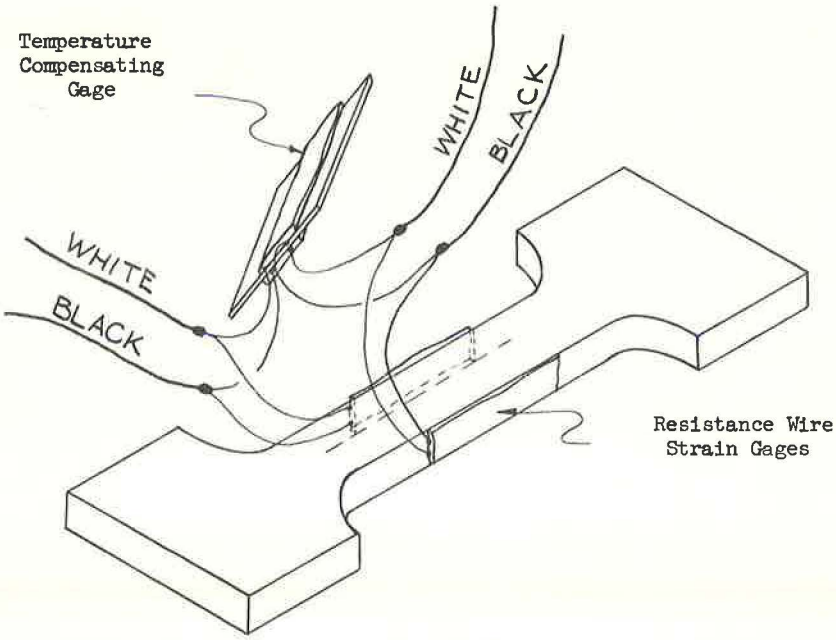

Figure 7. Towing test strain gage towbar.

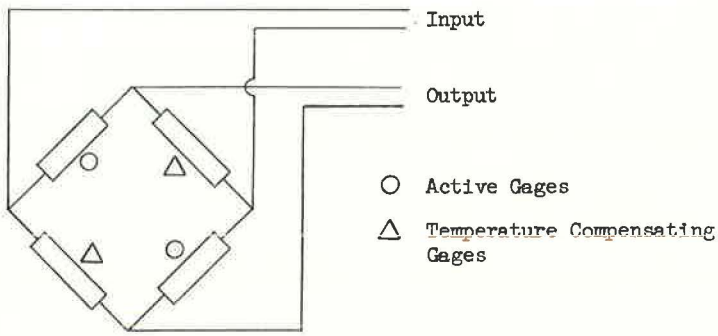

Figure 8. Schematic strain gage wiring.

indicator reading and the towbar calibration coefficient. The zero load strain indicator reading was read at the start and end of each separate experiment and was found to drift only slightly from day to day. The towbar was recalibrated periodically during the experiments but the calibration coefficient did not change measurably.

Tire dolly air drag force was calculated by subtracting the product of dolly weight and test section slope from the towbar force measured during the flatbed tests:

$$F_{AD} = F_M - (GVW)\left(\frac{G}{100}\right) \tag{1}$$

The results of these calculations (Fig. 9) show the variation of tire dolly air drag force, F_{AD}, with speed. This air drag force fits the usual drag force equation very well with a calculated drag coefficient, C_D, of 0.705 which appears reasonable:

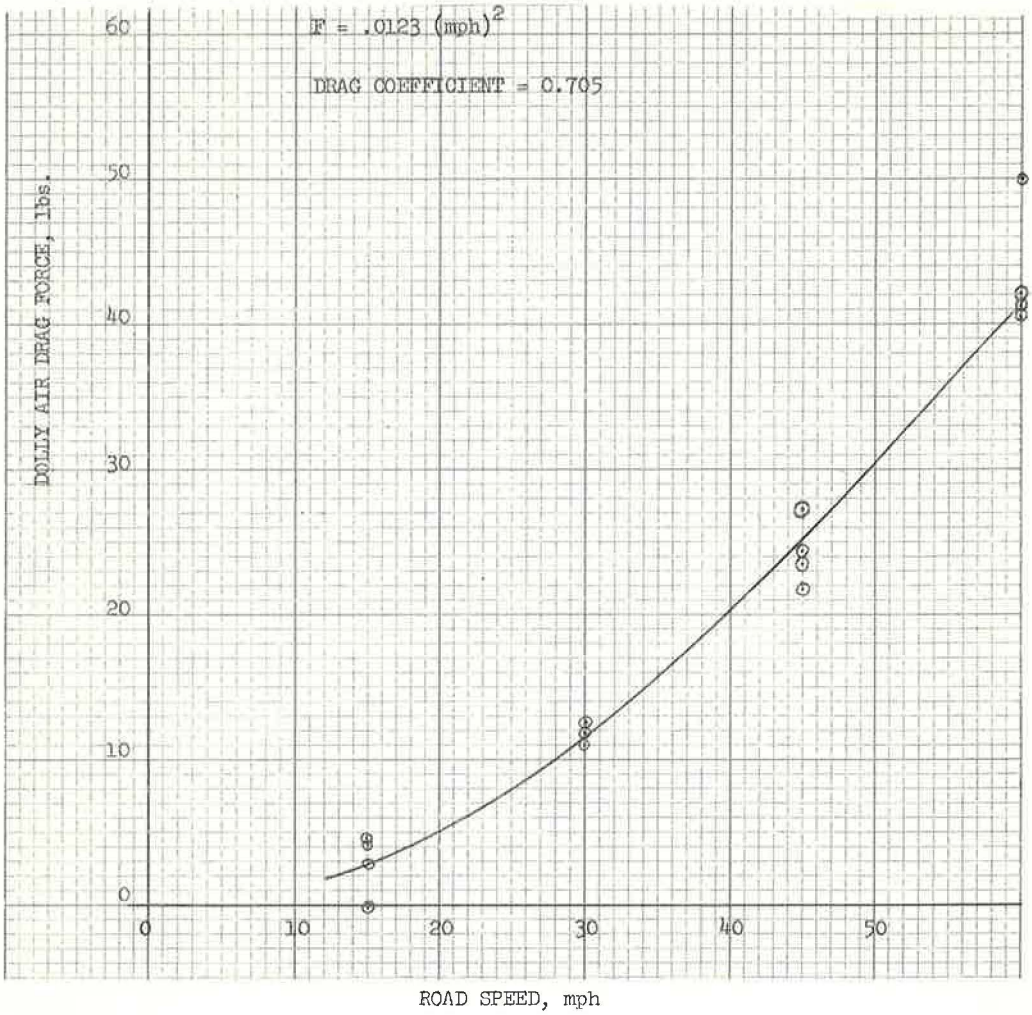

Figure 9. Tire dolly air drag force, averaged results.

$$F_{AD} = C_D A_F \rho_a \frac{V^2}{2g} = 0.0123 \text{ (mph)}^2 \tag{2}$$

Tire drag force was calculated by subtracting the air drag force, F_{AD}, and the slope force (product of dolly weight and test section slope) from the towbar force measured during the tire dolly towing tests:

$$2F_T = F_M - F_{AD} - (GVW)\left(\frac{G}{100}\right) \tag{3}$$

The results of these calculations (Figs. 10 through 13) show the variation of tire drag force per tire, F_T, with tire load speed.

The observed tire air temperature rise above ambient is plotted against tire load at various speeds in Figures 14 through 17. The observed tire tread temperature rise over ambient varied in essentially the same manner as for the tire air temperature rise but the tread data were more scattered.

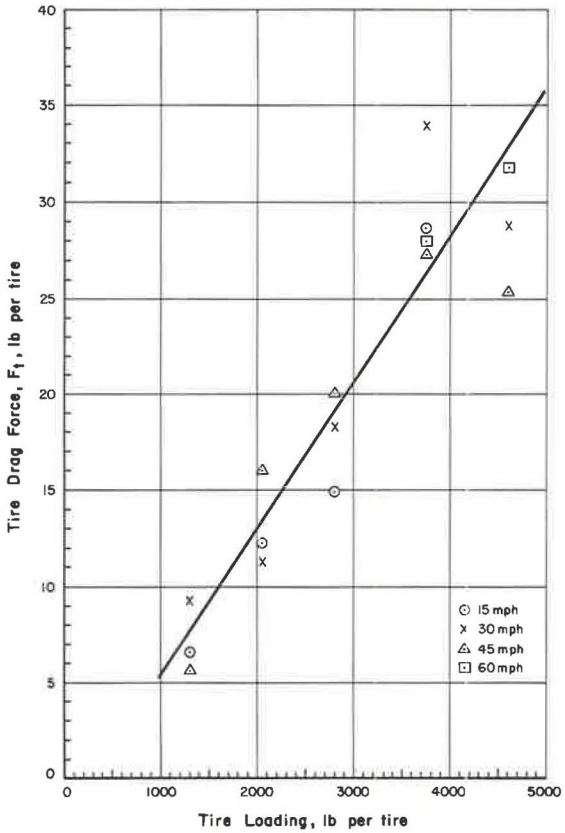

Figure 10. Tire drag force data, steel cord tires at 60 psig, 10:00-20.

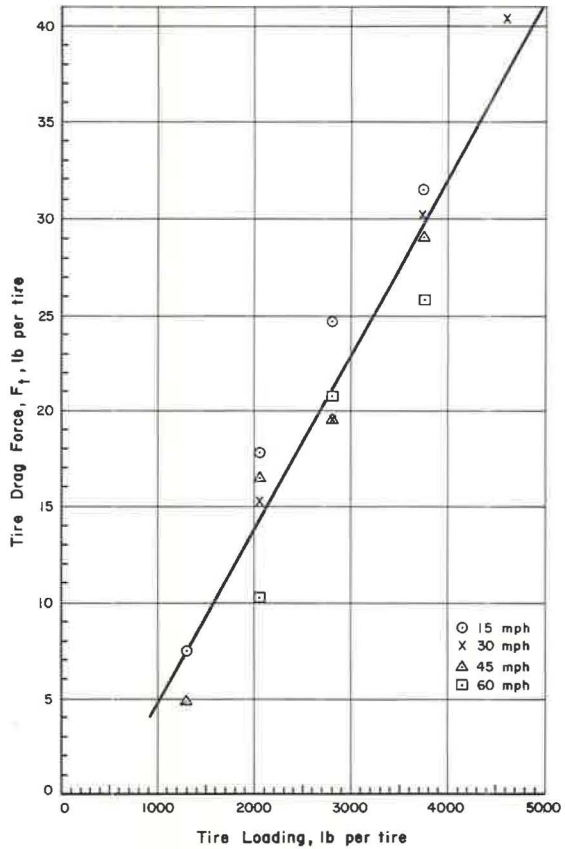

Figure 11. Tire drag force data, steel cord tires at 75 psig, 10:00-20.

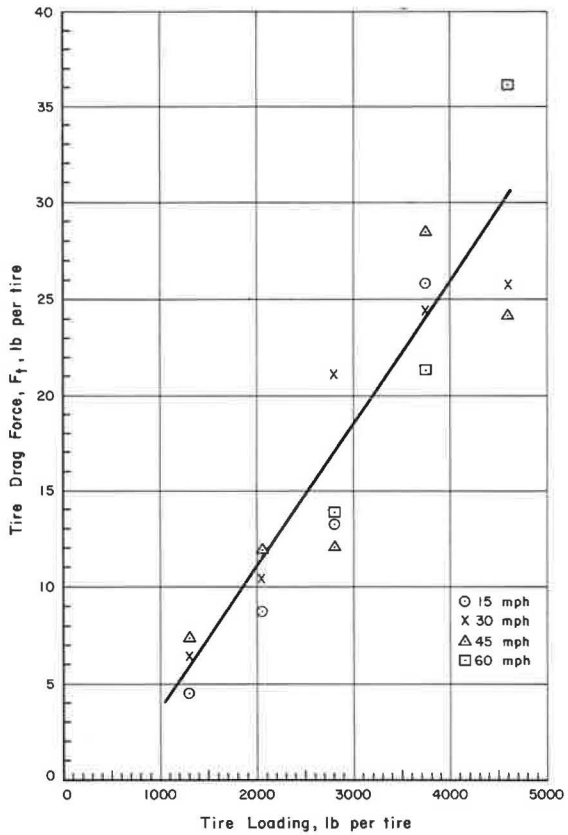

Figure 12. Tire drag force data, steel cord tires at 90 psig, 10:00-20.

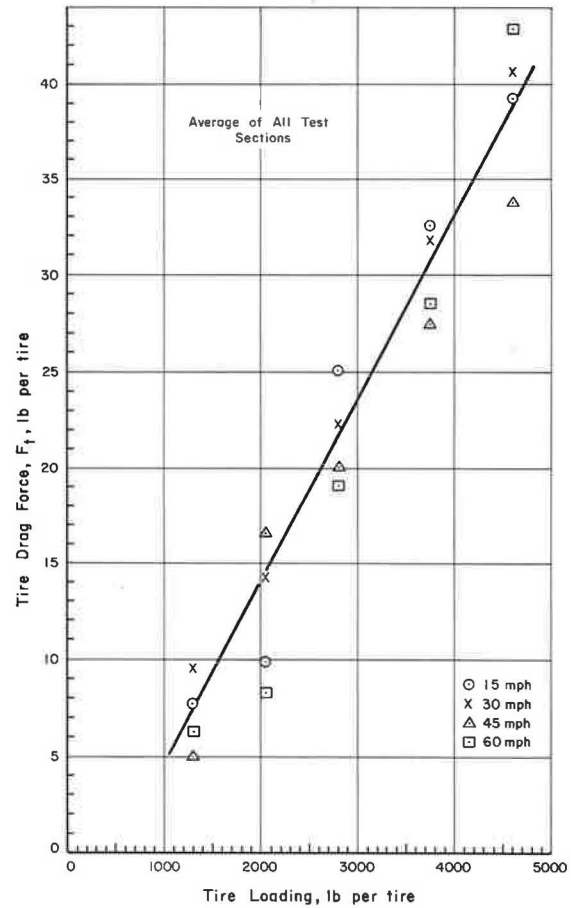

Figure 13. Tire drag force data, rayon cord tires at 75 psig, 10:00-20.

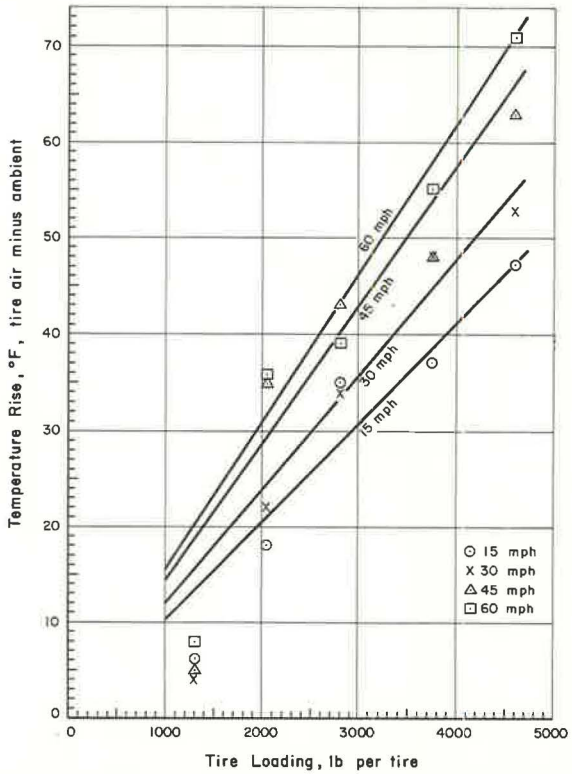

Figure 14. Tire temperature rise data, steel cord tires at 60 psig, 10:00-20.

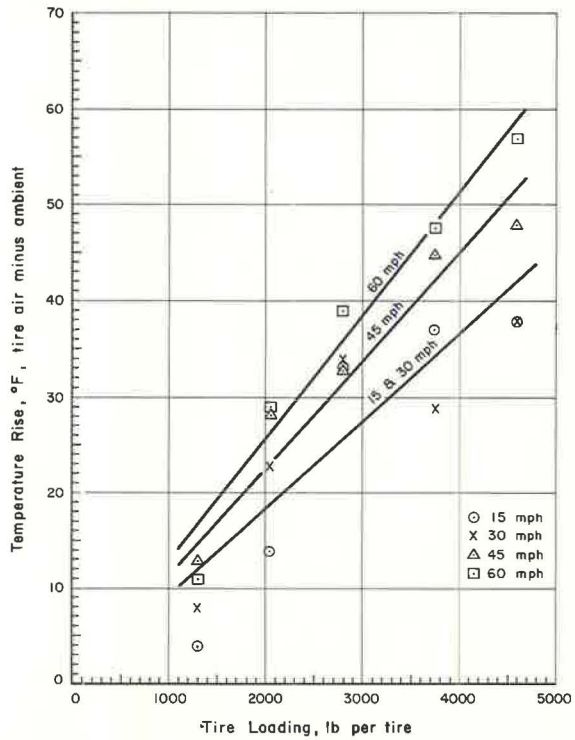

Figure 15. Tire temperature data, steel cord tires at 75 psig, 10:00-20.

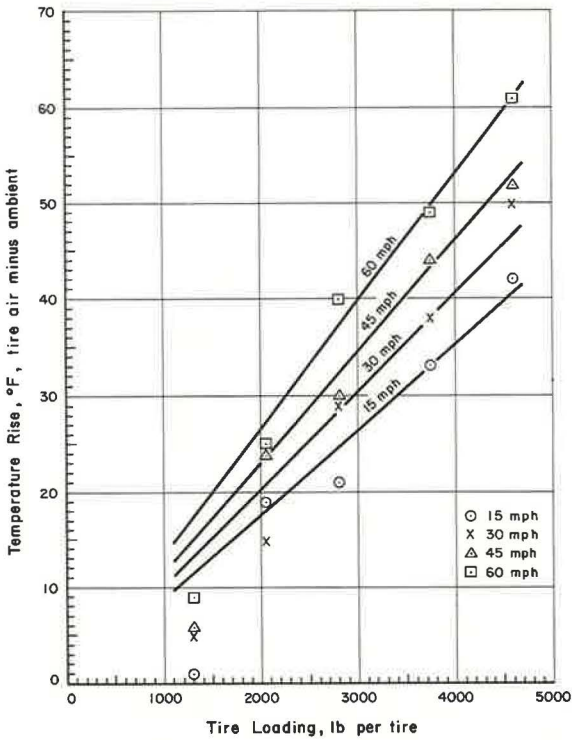

Figure 16. Tire temperature data, steel cord tires at 90 psig, 10:00-20.

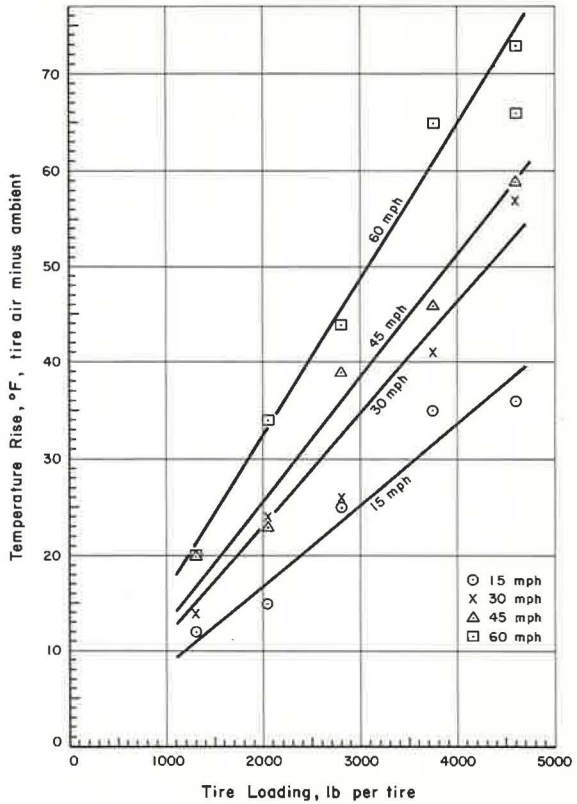

Figure 17. Tire temperature data, rayon cord tires at 75 psig, 10:00-20.

Truck Towing Tests

One of the test trucks was towed via the same bracket as used with the tire dolly towing tests. The test truck was towed at steady speeds between 30 and 45 mph and the towing force was recorded on the staked test sections. Tests were limited to this narrow range of speeds because at lower speeds steady towing force readings were difficult to obtain and higher speeds were considered unsafe. After running some of these towing tests it became apparent that towing tests on large trucks are unsafe at any speed on a public highway where unexpected sudden stops may be required. Accordingly only a limited amount of truck towing data was obtained. A comparison is shown in Figure 18 between total drag force as measured by the truck towing test and that as measured by the coastdown test. Both test methods give essentially the same answer. Further measurements of total drag force of the test trucks were made by coastdown tests only.

Coastdown Tests

The coastdown test (3, 4) consists of bringing the truck up to a speed of about 60 mph, disengaging the clutch and recording speed and time as the truck coasts to a stop. During the coastdown, the truck kinetic energy is being used to overcome the total drag force, which can be calculated from the rate of loss of kinetic energy. To obtain improved accuracy the following detailed changes were made in the test procedure of Sawhill and Firey (4):

1. A special calibrated speedometer indicating head driven by the truck speedometer cable was used instead of the usual truck speedometer or a fifth wheel. The gearbox

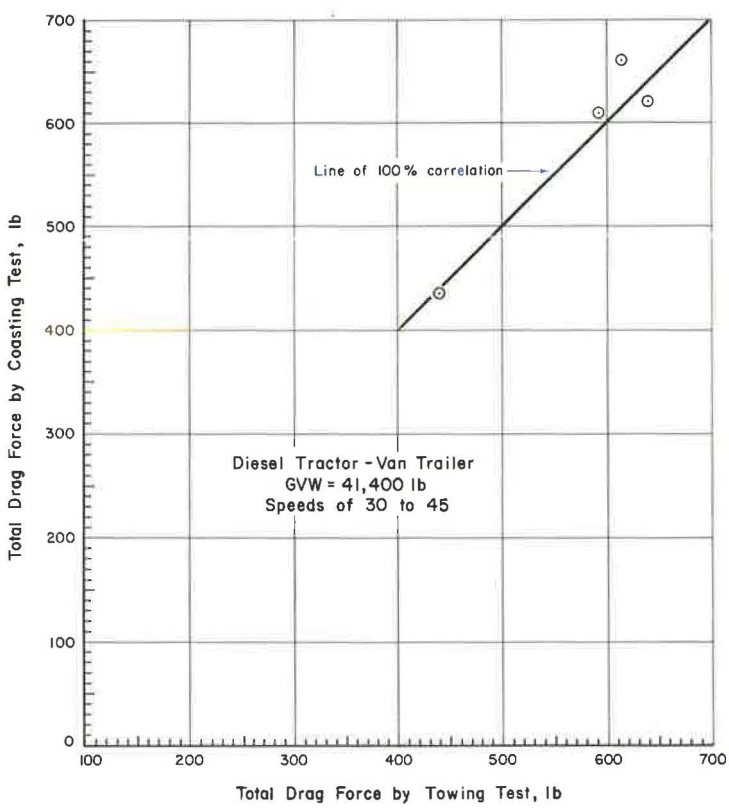

Figure 18. Comparison of total vehicle drag force as measured by coasting and towing tests.

between the speedometer cable and the indicating head was selected for each truck so that true speed was indicated. The special indicating head was more readable and more accurate than the truck speedometer. By using the truck speedometer cable the problem of fifth wheel bouncing was avoided.

2. The tests were run only on the staked test sections of known and uniform grade so that corrections for slope could be made accurately. Because these test sections were short, the full coastdown was done in two or more parts. In previous coastdown tests, the full coastdown was run at once and invariably a change of grade occurred somewhere during the test and only an approximate correction could be made for slope. Even a small error in grade correction can introduce a large error in total drag force.

3. Mr. Carl Saal suggested the use of a half-silvered glass with one edge straight for determining the position of the line tangent to the graph of truck speed vs time. The slope of this tangent line gives the truck deceleration and, hence, the total drag force. A half-silvered glass was not only a more accurate but also a more convenient means for determining the tangent line than the previous straightedge method.

When coasting on a grade, truck kinetic energy is utilized to overcome total drag force and to increase truck potential energy:

$$\frac{d(KE)}{dt} = F_D V + (GVW)\left(\frac{G}{100}\right) V \tag{4}$$

After introducing the kinetic energy equations and rearranging the units this relation becomes (4)

$$\frac{GVW}{29.6 \times 10^6}\left[1 + 128\,\frac{(W + 1)}{GVW}\right](mph)\left(\frac{\Delta mph}{\Delta T}\right) = \frac{F_D}{375}(mph) + \left(\frac{GVW}{375}\right)\frac{G}{100}(mph) \tag{5}$$

Solving for the total drag force, F_D, yields

$$\frac{F_D}{375} = \frac{RHP}{mph} = \frac{GVW}{29.6 \times 10^6}\left(\frac{\Delta mph}{\Delta T}\right) + \frac{128\,(W + 1)}{29.6 \times 10^6}\left(\frac{\Delta mph}{\Delta T}\right) - \frac{GVW\ (G)}{37,500} \tag{6}$$

On the right side of Eq. 6 the first term is the truck deceleration force, the second term is the wheel deceleration force, and the third term is the force due to grade. The truck deceleration was measured from the slope of the speed vs time graph during coastdown. Values of the total drag force, calculated in this manner, are plotted as the total drag force vs gross vehicle weight at constant speeds (Figs. 19 through 22) and as the total drag force vs the square of truck speed at constant gross vehicle weights (Figs. 23 through 26).

The linear increase of total drag force with increasing weight at constant speed can only be due to change of tire drag force because the air drag properties of the truck are not changed by weight. By assuming tire drag to be zero at zero load, as indicated by the tire dolly towing test results, the tire drag force can be calculated at each speed from the slope of the total drag force vs vehicle weight graphs:

$$F_T = 375\ (GVW)\ (slope),\ lb \tag{7}$$

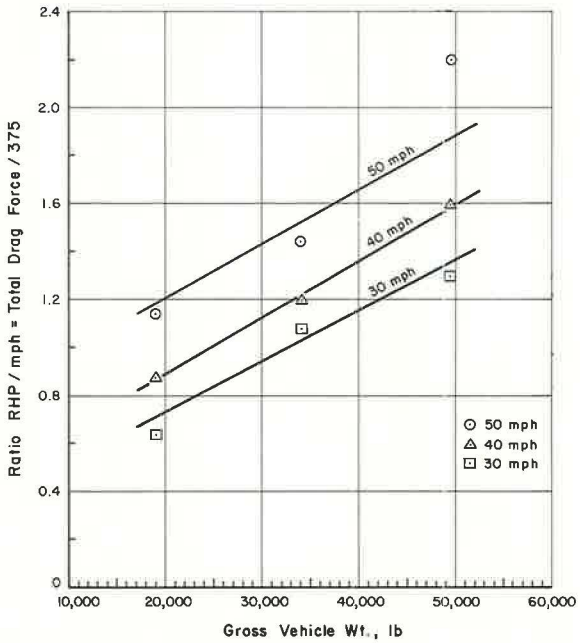

Figure 19. Total vehicle drag force by coasting test vs vehicle weight, gasoline tractor with flat-bed trailer.

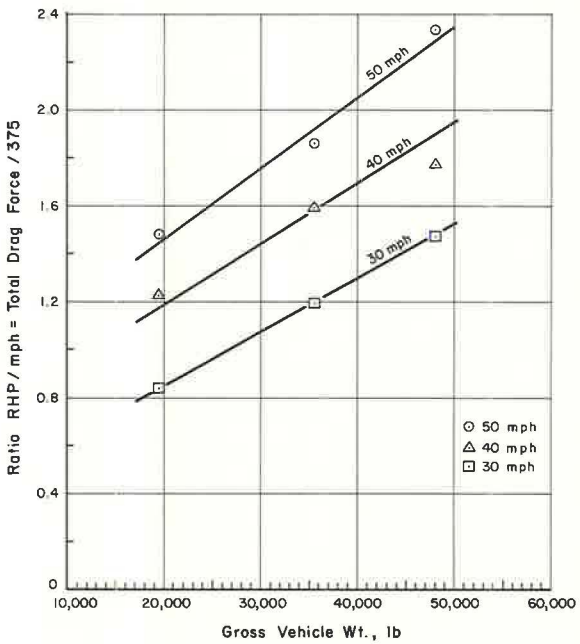

Figure 20. Total vehicle drag force by coasting test vs vehicle weight, gasoline tractor with van trailer.

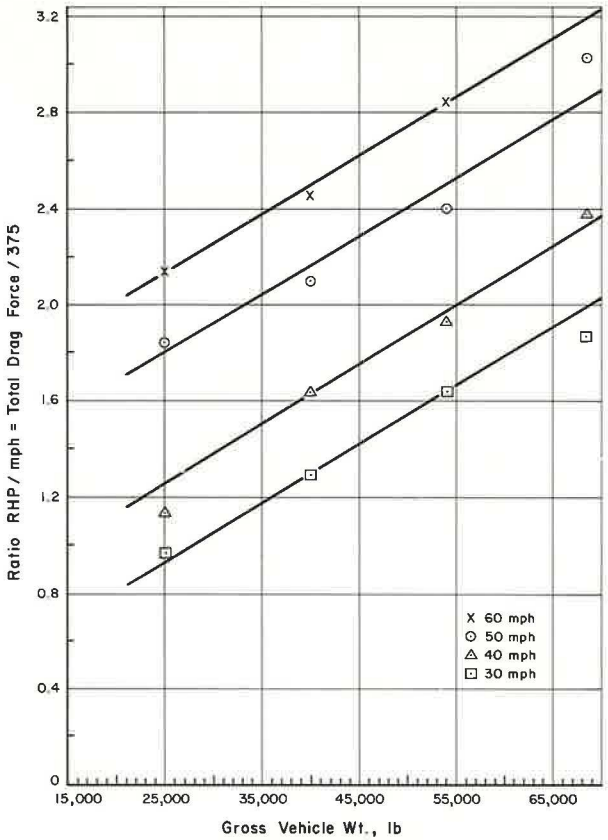

Figure 21. Total vehicle drag force by coasting test vs vehicle weight, diesel tractor with flat-bed trailer.

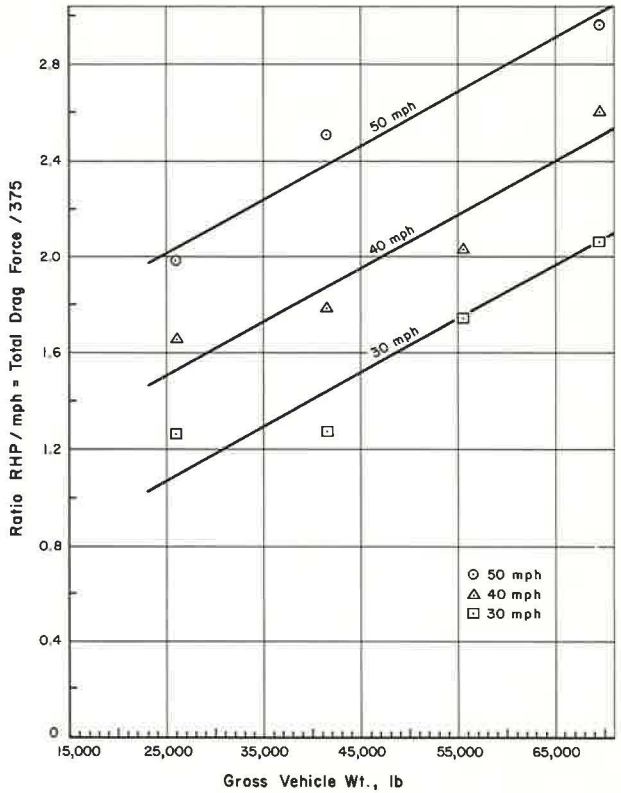

Figure 22. Total vehicle drag force by coasting test vs vehicle weight, diesel tractor with van trailer.

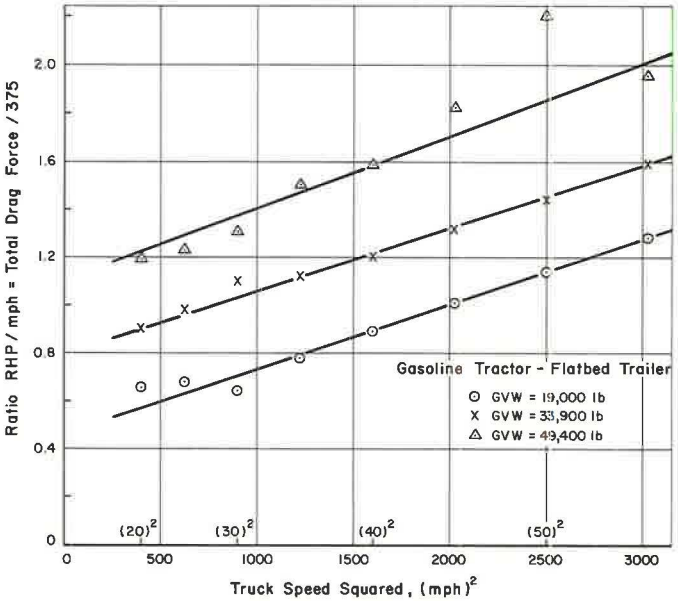

Figure 23. Total drag force vs speed squared.

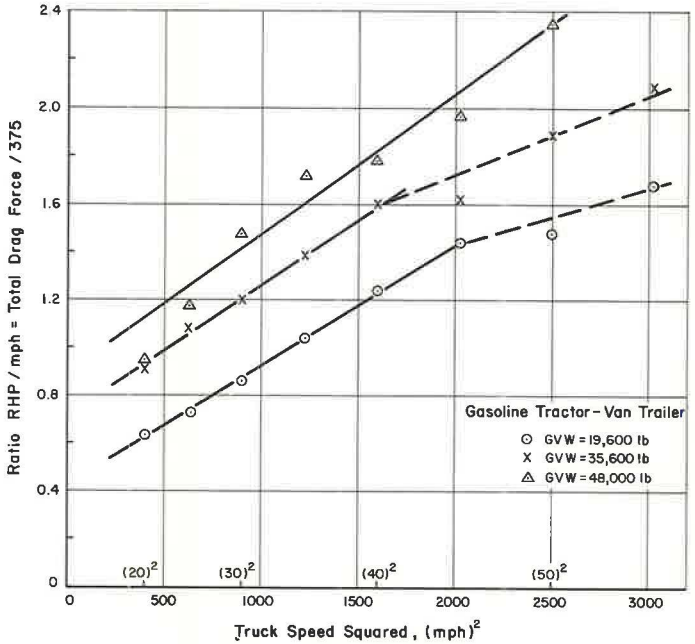

Figure 24. Total drag force vs speed squared.

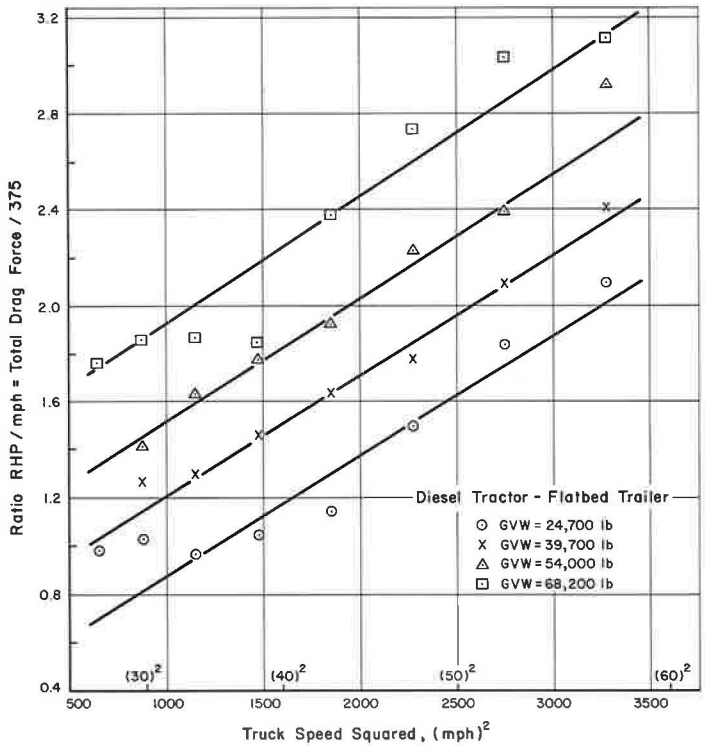

Figure 25. Total drag force vs speed squared.

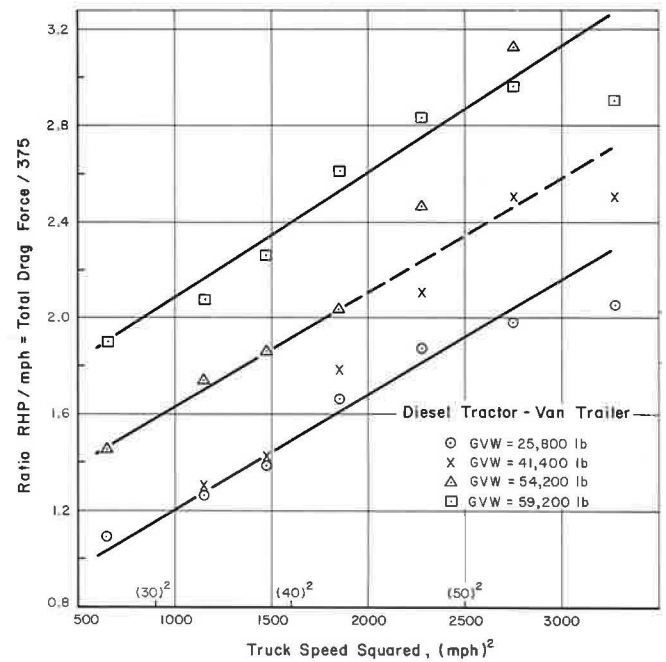

Figure 26. Total drag force vs speed squared.

in which the slope is in units of RHP/[(mph) (GVW)]. Tire drag force is also calculated in units of specific tire drag force, f_t, in pounds drag per 1,000-lb load. Tire drag force of the rayon cord test tires, calculated in this manner, was essentially independent of truck speed (Fig. 27). This result is in aggrement with the data obtained by the tire dolly towing tests shown in Figure 13. For the rayon cord tires tested, the coastdown tests gave an average specific tire drag force of 8.20 lb per 1,000 load, which agrees closely with the average specific tire drag force of 8.25 lb per 1,000 lb load obtained from the tire dolly towing tests.

The increase of total drag force with speed at constant load was presumed to result from the change of air drag force. This is equivalent to assuming tire drag force to be independent of speed as is shown in Figures 10 through 13. Air drag force was then calculated from the slope of the total drag force vs speed squared graphs:

$$F_A = 375\ (\text{mph})^2\ (\text{slope}),\ \text{lb} \tag{8}$$

in which the slope is in units of RPH/(mph)^3.

The air drag coefficient, C_D, was calculated for each vehicle by fitting the air drag force to an air drag equation:

$$F_A = C_D A_F \frac{\rho_a V^2}{2g} \tag{9a}$$

$$C_D = \frac{2gF_A}{A_F \rho_a V^2} \tag{9b}$$

The truck air drag coefficients, calculated in this manner, are given in Table 3.

This method for separately determining tire drag force and air drag force from coastdown tests is essentially that described by Beck (5) and is equivalent to assuming

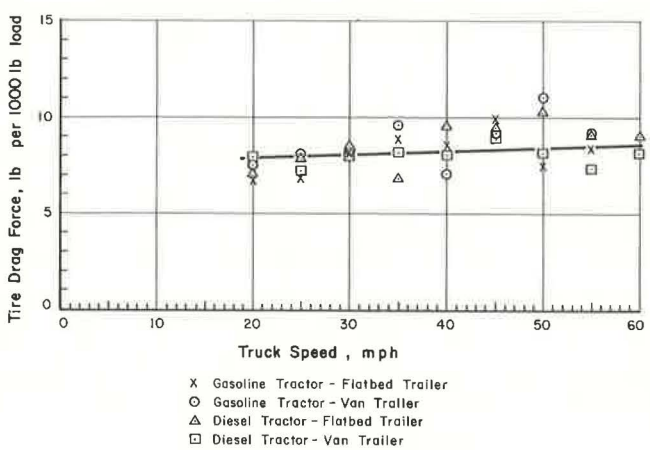

Figure 27. Tire drag force by coasting test vs truck speed, rayon cord tires at 75 psig, 10:00-20.

TABLE 3

TEST VEHICLE AIR DRAG COEFFICIENTS

Vehicle	C_D
Gasoline tractor, flatbed trailer	0.835
Gasoline tractor, van trailer	0.873
Diesel tractor, flatbed trailer	1.240
Diesel tractor, van trailer	0.813

total drag force consists of a weight dependent term, the tire drag force, and a speed squared dependent term, the air drag force:

$$F_D = F_T + F_A = GVW \frac{f_t}{1,000} + C_D A_F \left(\frac{\rho_a V^2}{2g}\right) \qquad (10)$$

The following assumptions are implied in using this calculation procedure: (a) the tire drag force is zero at zero load; (b) it is independent of speed; (c) it increases linearly with load; and (d) gear and bearing friction in the drive train and wheels is negligible. Assumptions (a), (b), and (c) are approximately verified for the rayon cord tires by the tire dolly towing test results shown in Figure 13. By the foregoing calculation method the gear and bearing friction force is split into two parts, the load dependent part being included with the tire drag force and the speed dependent part being included with the air drag force. Future experiments are planned to measure separately the gear and bearing friction force.

Wheel Tests with a Torsional Spring

Part of the truck kinetic energy, calculated in the coastdown tests, is translational and part is rotational. The translational kinetic energy is calculated from the measured speed and weight. The wheel polar moment of inertia is needed to calculate the rotational kinetic energy. In previous studies (4) an estimated value of wheel moment of inertia was used. In this work the wheel moment of inertia is directly measured by coupling the wheel to a torsional spring and measuring the natural frequency of torsional vibration of the system. Details of this torsional spring unit are shown in Figure 28. The spring was a ½-in. steel bar of 24-in. length having a spring constant of 3,070 lb-in. torque per radian. To measure the oscillations of the wheel, four strain gages were mounted on the spring at 45° to the axis. By mounting two gages 180° apart on a right-hand helix and two gages similarly on a left-hand helix, the effects of bending, axial loads and thermal expansion were minimized. The test wheel was jacked up, connected to the spring and given an initial rotation of 25°. The decaying wheel oscillations were sensed by the strain gages and the imbalance of the gage bridge circuit was recorded on a strip chart recorder. From the strip chart record the natural frequency, or vibration cycle period, of the wheel and spring system was measured. The wheel polar moment of inertia was then calculated by use of the usual torsional vibrational relation:

$$I = \frac{p^2 K}{4\pi^2} \qquad (11)$$

If the effect of damping (assumed viscous) is included the more accurate relation becomes

$$I = \frac{P^2 K}{4\pi^2 + R^2} \qquad (12)$$

Damping was calculated by measuring the decrease in oscillation amplitude from one cycle to the next:

$$R = \log\left(\frac{\Theta_1}{\Theta_2}\right) \qquad (13)$$

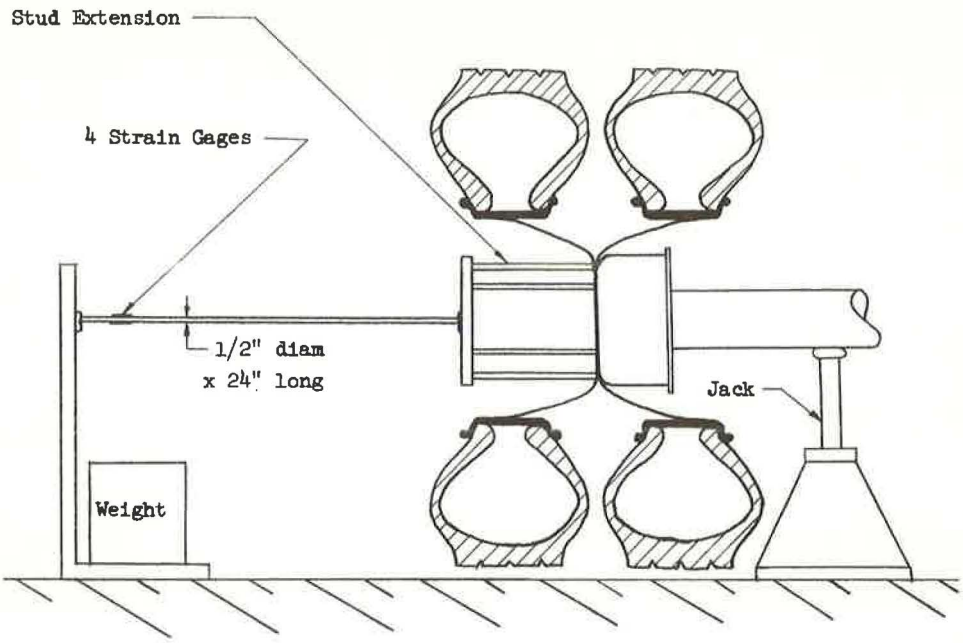

Figure 28. Wheel torsional spring unit.

Several sets of dual wheels were tested with the following average results: period = P = 1.81 ± 0.02 secs; damping = R = 0.40; and Polar moment of inertia = I 258 lb-in.-sec^2 for two wheels and rims with 10:00-20 tires and a brake drum. Extreme accuracy is not ordinarily needed in determining the wheel polar moment of inertia because rotational kinetic energy of a large truck is only between 5 and 10 percent of the total kinetic energy.

DISCUSSION

Tire Drag Force

Tire drag force appears to originate largely from hysteresis of the tire rubber. The rubber in the tire tread is bent through an angle, Φ, as the tread enters the flattened part on the road. This deflection produces stresses in the rubber and work is done on the rubber. Due to the nature of rubber only a part of this work is recovered when the tread rubber unbends on leaving the flattened part. The loss in work produces both the tire drag force and internal heating and temperature rise within the tire.

The following rather crude analysis of tire deflections may serve to indicate qualitatively some of the factors which influence tire drag force. The angle, Φ, through which the tread rubber is bent is related to the length, l, of the flattened portion as

$$\Phi = \frac{l}{2r} \tag{14}$$

The total work done in thus bending the tread rubber varies directly with Φ and the volume of rubber bent:

$$\text{Work} = c\,\Phi b\,d\ (\text{velocity})\ (\text{time}) \tag{15}$$

$$\text{Volume} = b\,d\ (\text{velocity})\ (\text{time}) \tag{16}$$

A constant fraction, h, of this work is lost internally to hysteresis:

$$\text{Lost Work} = h\,c\,\Phi\,b\,d\ (\text{velocity})\ (\text{time}) \tag{17}$$

This lost work should equal the product of tire drag force, F_t, truck velocity and time:

$$\text{Lost Work} = F_t\ (\text{velocity})\ (\text{time}) \tag{18}$$

$$F_t = h\,c\,\Phi\,b\,d = \frac{h\,c\,l\,b\,d}{2\,r} \tag{19}$$

The area, A_t, of the flattened portion is approximately equal to the ratio of load, W, to inflation pressure, p_i:

$$A_t = \frac{W}{p_i} \tag{20}$$

This area is also equal to a constant, a, times the length, l, and width, b, of the flattened portion:

$$A_t = a\,l\,b = \frac{W}{p_i} \tag{21a}$$

$$l\,b = \frac{W}{a\,p_i} \tag{21b}$$

$$F_t = \frac{W\,h\,c\,d}{2\,a\,r\,p_i} \tag{22}$$

An approximate experimental verification of this relation is found in the following observations:

1. Tire drag force increases very nearly linearly with tire load (Figs. 10 through 13).
2. Tire drag force usually decreased at higher inflation pressure (Figs. 10 through 12), although the effect was not as large as indicated by Eq. 22.
3. Measurements were made of the area of the flattened portion for the rayon cord tires at 75 psig inflation pressure. The product of inflation pressure and flattened area equaled applied load within about 20 percent.
4. Previously reported experiments (6) suggested that worn tires, having a smaller tread thickness, d, showed lower values of tire drag force.

Eq. 22 can only be very approximate because many complicating factors, such as deflections of the sidewall rubber and variations of a with load, were not considered. Nevertheless, this analysis appears to provide a qualitatively correct picture of the origin of the tire drag force.

The portion of the tire tread bending work lost to hysteresis reappears as increased tire and tire air temperature. Presumably at equilibrium tire temperature, the rate of hysteresis work equals the power required to overcome tire drag force and also equals the rate of heat transfer from the tire to the ambient air:

$$F_T \text{ (velocity)} = \text{hysteresis power} = \frac{dQ}{dt} \tag{23}$$

$$F_T \text{ (velocity)} = UA_x (T_t - T_a) = UA_x \Delta T_t \tag{24}$$

Because ΔT_t is the tire temperature rise above ambient by definition:

$$\Delta T_t = \frac{F_T \text{ (velocity)}}{UA_x} = \frac{Whcd \text{ (velocity)}}{2UA_x \, arp_i} \tag{25}$$

This relation predicts that tire temperature rise increases linearly with load as was observed experimentally (Figs. 14 through 17). The observed effects of tire inflation pressure, p_i, and truck speed on tire temperature rise Figs. 14 through 16) agree qualitatively but not quantitatively with Eq. 25. The relatively small effect of velocity on tire temperature rise may result from an increase of heat transfer coefficient, U, from tire to ambient air due to increased velocity. Turbulent flow heat transfer coefficients increase with about the 0.8 power of velocity. Hence, tire air temperature rise should then increase with about the 0.2 power velocity, as was indeed observed for the data of Figures 14 through 17.

Interest in tire tread and tire air temperatures originally centered around the thought that the rubber hysteresis coefficient, h, varied with rubber temperature, being generally lower at higher temperature. Hence, at higher load, tire drag force would not be proportionately increased because tire temperatures would be greater. Because the experimental results show tire drag force to increase nearly linearly with tire load it would appear that variations of the rubber hysteresis factor with temperature are small within the range of temperatures of these experiments (70 to 140 F).

The tire drag force data reported herein do not agree very well with previous data on truck tires reported by Stiehler et al. (7). Stiehler measured tire drag force in a laboratory apparatus by running the test tires against a steel drum of about 5.5 ft diameter. Both sets of results agree on the effect of load except that Stiehler shows that an appreciable tire drag force exists at zero load. It is difficult to reconcile the two sets of results except on the possible basis that a tire deflects very differently against the steel drum than it does against a flat highway surface.

Air Drag Force

The air drag force of a truck results from skin friction drag over the entire external surface area of the truck and pressure drag due to air displacement by the frontal area of the truck. For passenger cars, pressure drag appears to be much larger than skin friction drag (8). Presumably this is also true for large transport trucks, although very little experimental data are published concerning the air drag properties of large trucks. Judging from experimental results on passenger cars and car models (8) a significant portion of motor vehicle drag results from protuberances such as rear view mirrors, and door knobs, and particularly from protuberances on the underside such as springs and axles. This protuberance drag is primarily pressure drag.

For truck speeds greater than about 30 mph the air drag coefficients, C_D, as measured by these road test methods are in reasonable agreement with air drag coefficients for truck models as measured by Flynn and Kyropoulos in wind tunnel tests (1).

Some of the uncertainties about the true air drag of full-scale trucks are expected to be resolved by the forthcoming railroad flatcar tests of truck air drag and the wheel spinning tests of bearing and gear friction. For the railroad flatcar tests, the test trucks will be suspended on flatcars and the air drag force measured in a manner similar to that used for measuring the tire dolly air drag force. To measure bearing friction a nondrive wheel is spun up and speed and time recorded as the wheel coasts to a stop. During the coastdown, wheel rotational kinetic energy is utilized to overcome bearing drag which can be estimated from the rate of loss of kinetic energy. A similar

experiment on a set of drive wheels will permit estimation of the gear and drive train friction. It is hoped that the air drag results obtained by coasting test, when corrected for bearing and gear drag, will agree fairly closely with the air drag results obtained by railroad flatcar test.

Application to Fuel Consumption and Travel Time Estimation Procedures

The results reported herein indicate that truck rolling resistance can be closely approximated as being composed of a speed squared dependent term, the air drag, and a gross vehicle weight dependent term, the tire drag. In the fuel consumption analysis of Sawhill and Firey (2) truck rolling resistance was assumed to depend only on gross vehicle weight. The analysis method used cannot be readily modified to include correctly the air drag effect. This limitation applies also to their travel time analysis, because the fuel consumption calculation is an integral part of the travel time estimation procedure. Perhaps some of the discrepancies noted by Sawhill and Firey between their theoretical and empirical fuel consumption analyses resulted from the incorrect rolling resistance relation used.

The difficulty originates from the necessity of knowing the truck speed before the air drag force can be estimated. The truck speed, in turn, is to some extent dependent on the magnitude of the air drag force. An approximate way out of this dilemma appears to lie in the following method for fuel consumption and travel time estimation for a particular truck on a specified section of highway:

1. The maximum speed-distance-time history of the truck on the highway can be estimated by assuming the truck to be at legal speed limit or, where this cannot be maintained, at maximum sustained speed as calculated by the methods of Firey and Peterson (9). The travel time is now directly calculable.
2. With speeds known the various drag forces can be determined, as well as the duration of wide-open throttle running, and hence, the fuel consumption can be calculated by the methods of Sawhill and Firey (2) modified to include an air drag power term.

Although the details of this calculation procedure remain to be worked out, it appears likely that it will be a more cumbersome calculation than the relations developed earlier. However, the proposed calculation procedure can probably be used with greater confidence in predicting the effects of future truck and highway designs on fuel consumption and travel time.

ACKNOWLEDGMENTS

The writers wish to express their appreciation of the generous financial assistance given this research by the U. S. Bureau of Public Roads under Research Contract CPR 11-8016. The cooperation and assistance given by the Washington State Highway Department and the Washington State Patrol are also appreciated.

REFERENCES

1. Flynn, H., and Kyropoulos, P., "Truck Aerodynamics." SAE Preprint 284A (Jan. 1961).
2. Sawhill, R. B., and Firey, J. C., "Predicting Fuel Consumption and Travel Time of Motor Transport Vehicles." HRB Bull. 334, pp. 27-46 (1962).
3. Saal, C., "Public Roads." (May 1942).
4. Sawhill, R. B., and Firey, J. C., "Motor Transport Fuel Consumption Rates and Travel Time." HRB Bull. 276, pp. 35-91 (1960).
5. Beck, W., "An Investigation of Motor Vehicle Parasitic Power Loss by Road Test." M. S. in M. E. Thesis, Univ. of Washington (1962).
6. Firey, J. C., "Effects of the Tire Pressure and Temperature on the Rolling Resistance of Trucks." Univ. of Washington, Traffic and Operations Series, Transportation Res. Group, Res. Rep. 4 (June 1962).
7. Stiehler, R. D., Steel, M. N., Richey, G. G., Mandel, J., and Hobbs, R. H.,

"Power Loss and Operating Temperature of Tires." Jour. Res. NBS, 64C: 1 (Jan.-Mar. 1960).

8. Hoerner, S. F., "Fluid Dynamic Drag." Midland Park, N. J., pp. 12-1—12-9 (1958).
9. Firey, J. C., and Peterson, E. W., "An Analysis of Speed Changes for Large Transport Trucks." HRB Bull. 334, pp. 1-26 (1962).
10. "Truck Ability Prediction Procedure." SAE Rec. Prac. Rep. TR-82.